Determination of the strain-optical parameters for a polarimetric optical sensor embedded in a composite laminate

H. Wang[1], S.L. Ogin[1], A.M.Thorne[1], G.T. Reed[2] and M Ussorio[1]

[1]*School of Engineering*
[2]*School of Electronics and Physical Sciences*
University of Surrey, Guildford, Surrey GU2 5XH, UK

Abstract

Polarimetric fibre optical sensors embedded in composite laminates are capable of detecting damage in the form of matrix cracking. To interpret the behaviour of the sensors when damage develops, it is first necessary to determine the strain-optical parameters of the sensor itself. In this work, the sensitivity of a bare polarimetric sensor manufactured from Hi-Bi PANDA fibre has been measured experimentally and a phase-strain model available in the literature has been used to determine the characteristic parameters of the optical fibre. The results suggest that a polarimetric sensor based on the PANDA fibre embedded in a composite laminate will be less sensitive to damage development than an equivalent sensor based on Bow-tie fibre.

1. Introduction

Polarimetric fibre optical sensors are sensors that have high lateral strain sensitivity. The high lateral strain sensitivity arises from the use of high birefringence (Hi-Bi) optical fibre that incorporates doped regions with a different coefficient of thermal expansion (called Stress Applying Parts, SAPs). Previous work has shown that when a polarimetric sensor is embedded in the 0° ply of a cross-ply composite laminate near the 0/90 interface, the sensor can detect transverse cracks in the 90° ply that pass the sensor [e.g. 1-2]. Hence the sensor has the potential to be used for damage detection in real engineering applications. In order to understand the response of such an embedded sensor to damage, it is necessary to determine the strain-optical parameters that relate the changes in strain to changes in the optical output, and a model developed by Sirkis [3] enables this to be achieved.

According to this model, the relative phase change between the two polarisation modes of the polarimetric sensor, $\Delta\varphi$, is given by:

$$\Delta\varphi = \frac{2\pi}{\lambda}\int_L [K_1\varepsilon_1 + K_2\varepsilon_2 + K_3\varepsilon_3]dL \qquad (1)$$

where $\Delta\varphi$ is the relative phase change between the two polarisation modes caused by the three-dimensional strain, λ is the wavelength of light in vacuum, ε_1, ε_2 and ε_3 are the three normal strains (where the 1-axis is parallel to the length of the sensor), and L is the gauge length of the sensor. K_1, K_2 and K_3 are dimensionless parameters to be determined which govern the contribution of each component of the normal strains to $\Delta\varphi$. The K values are characteristic parameters of the optical fibre and are determined by the interaction between the optical fibre core, the SAPs and the cladding, due to the differing thermal expansion coefficients of these regions. Previous work by Sirkis and colleagues [4,5] determined the K values for a polarimetric sensor using Bow-tie optical fibres. In the present study, the

polarisation-maintaining fibre used was Fujikura PANDA Hi-Bi fibre, for which the *K* values have not previously been determined (**Fig. 1** shows a cross-section of the PANDA Hi-Bi fibre embedded in a cross-ply composite coupon). These measurements have been carried out using a modification of the method used by Sirkis [5].

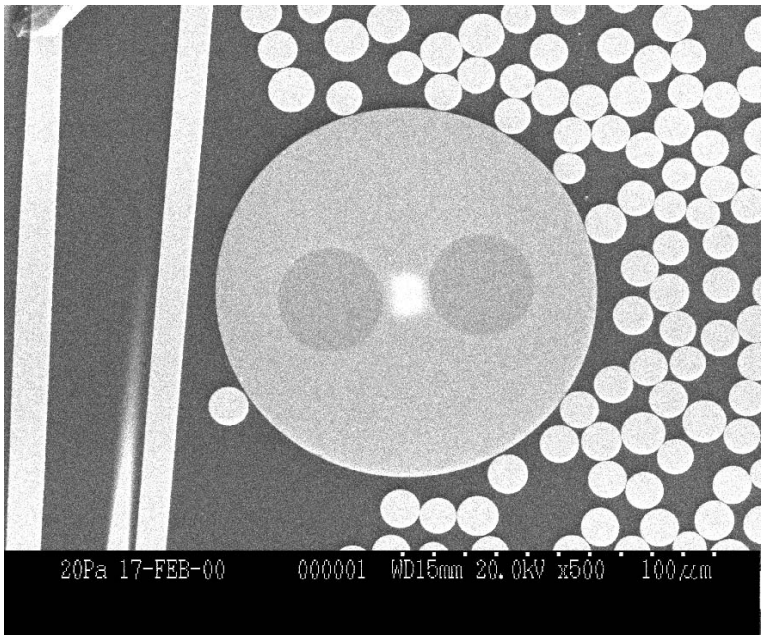

Fig. 1. A cross-section image of a PANDA fibre embedded in the 0^0 ply of a cross-ply composite coupon. The optical fibre diameter is 125 µm.

2. Experimental methods

The sensors were made of a single mode, polarisation maintaining fibre (Hi-Bi PANDA fibre obtained from Fujikura Europe Ltd), having a diameter without coating of 125 µm, a core diameter of 3.5 µm with SAP diameter of 16.5µm. A protective nylon coating and inner silicone coating were removed from the fibre by a coating stripper and a lens tissue soaked with high purity alcohol (to clean the stripped bare fibre). As shown in **Fig. 2**, the gauge length of the polarimetric sensor was achieved in the normal way by a rotation of the axes of the fibre through 45° at each of two splices, relative to the orientation of the lead-in/lead-out sections of the optical fibre. Splicing and rotation of the fibres were carried out using a Fujikura fusion splicer (Model: FSM-20PM). The light source launched into the lead-in fibre was linearly polarised light generated from a He-Ne gas laser source with an operational wavelength of 633 nm; the lead-out fibre was connected to a photo amplifier by a standard connector. The output signal from the amplifier is converted to a voltage signal and recorded by a datalogger.

To determine the *K*-values, tensile and compression loads were applied to the stripped sensing length of the sensor by specifically manufactured rigs.

Tensile tests of free sensors were carried out in a specially made tension rig (see **Fig. 3**). The sensor was fastened to the frame by two grips, one of which is fixed. Displacement of the sensor was introduced by withdrawing plate A (which is attached to the second grip) using a micro-screw knob at a manually controlled speed. Strain on the sensor was calculated by

dividing the displacement of the plate by the length of the bare fibre between the two grips. The displacements could be measured to an accuracy of 0.02 mm using the micro-screw knob.

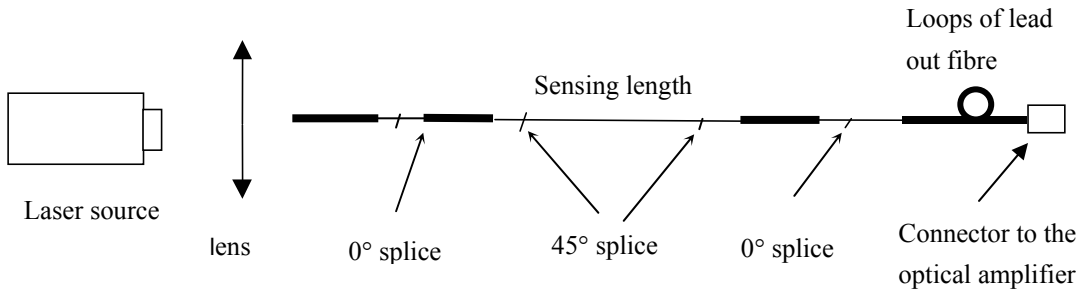

Fig. 2 Schematic figure showing the structure of a free sensor.

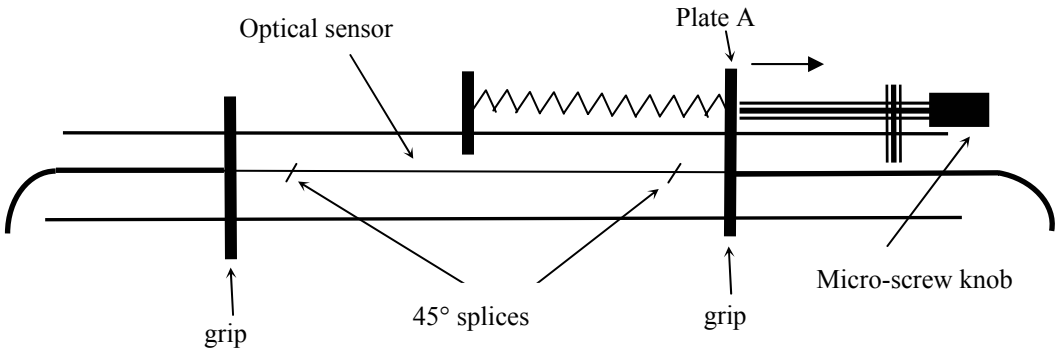

Fig. 3 Schematic of the tensile test of the free polarimetric sensor.

Transverse compression tests of the bare polarimetric sensors were carried out using manual loading. The experimental setup is shown in **Fig. 4**. Three flat gauge plates and an optical bench were used in the experiments to ensure a flat surface during the tests. In these compression experiments, the sensor must be rotated by known, controlled angles. To facilitate the rotation of the sensor by known amounts (increments of 15°), two optical chucks were used to grip the fibre and to control the rotation of the sensor. After rotating the fibre to the appropriate angle, the load was applied manually. A dummy bare fibre was used to share the compression load so that weights could be placed on the gauge plate, which was

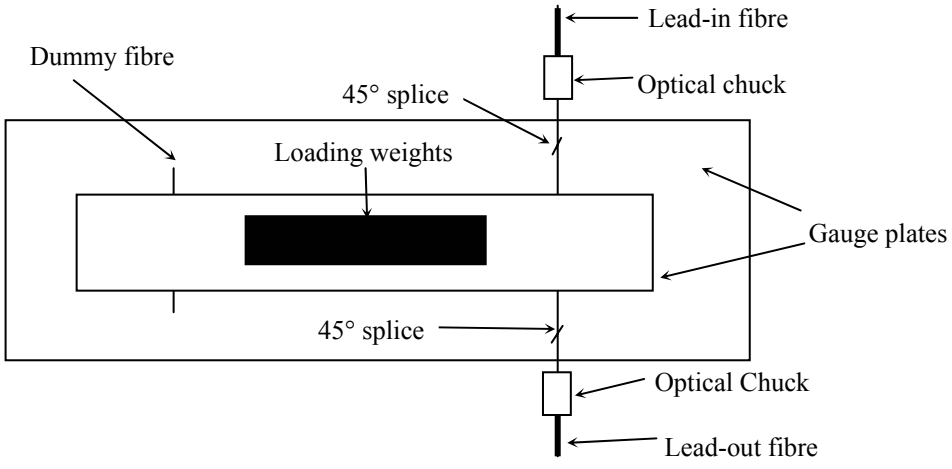

Fig. 4 Schematic of the compression test of the free polarimetric sensor.

positioned on top of the sensor, without tipping of the gauge plate. Ten weights, each 475 g, were placed onto the gauge plate by hand at regular intervals of about 4 seconds. In these experiments, a smooth increase in load is not necessary – it is the response of the sensor output to a well-defined load that is important. The width of the top gauge plate (the length of the sensor under transverse compression) was 20 mm. The optical output was recorded by the data-logger as a function of time and the resulting fringe profile was stepped because of the incremental increase in load. Results were taken for the optical fibre rotated by increments of 15°.

3. Experimental results

3.1 Experimental results of the tensile tests

When a free polarimetric sensor with structure shown in **Fig. 2** was strained in the tension rig shown in **Fig.** 3, the whole length of the fibre between the grips was under strain, and the gauge length of the sensor, L, is shorter than this length. Typical optical fringes obtained from the polarimetric sensor under tension are shown in Fig. 5. The fringes are shown as a function of time and although the displacement was controlled manually (and hence the frequency of the fringes is not constant), clear fringes are obtained from the sensors.

The longitudinal phase sensitivity of a bare fibre, S_{axial}, is defined as:

$$S_{axial} = \frac{1}{L}\frac{\Delta\varphi}{\Delta\varepsilon_1} \tag{2}$$

where L is the gauge length of the sensor, $\Delta\varphi$ is the change of phase and $\Delta\varepsilon_1$ is the longitudinal strain change. The transverse strains of a free sensor when it is under tensile load are given by:

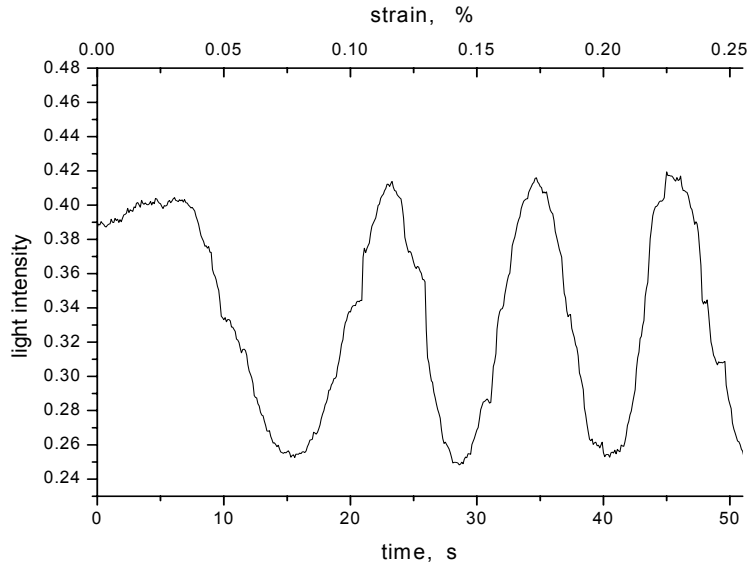

Fig. 5 Experimental results of free polarimetric sensor with structure shown in **Fig. 2**.

$$\varepsilon_2 = \varepsilon_3 = -\nu_f \varepsilon_1 \tag{3}$$

where ε_2 and ε_3 are transverse strains (as seen by the optical fibre's core), and ν_f is the Poisson's ratio of the optical fibre (ν_f = 0.154, here) . Combining with Eq.(1), the phase difference between the two modes in the core as a result of the applied longitudinal strain is:

$$\Delta\varphi = \frac{2\pi}{\lambda}\int_L [K_1\varepsilon_1 + K_2\varepsilon_2 + K_3\varepsilon_3]dL = \frac{2\pi}{\lambda} L\varepsilon_1(K_1 - \nu_f K_2 - \nu_f K_3) \quad (4)$$

Substituting Eq.(4) into Eq.(2), the longitudinal axial strain sensitivity becomes:

$$S_{axial} = \frac{1}{L}\frac{d(\varphi)}{d\varepsilon_1} = \frac{2\pi}{\lambda}(K_1 - \nu_f K_2 - \nu_f K_3) \quad (5)$$

Here, λ, ν_f, K_1, K_2 and K_3 are constants which depend on the laser source and characteristics of the optical fibre. Hence the longitudinal strain sensitivity of the sensor should be constant and independent of the gauge length of the sensor. The measured longitudinal strain sensitivity of the sensor was 106 ± 2 rad/mm, obtained from 5 experimental measurements, where the uncertainty is the standard deviation. The complete set of results, showing sensor gauge length and measured sensitivity, are shown in **Table 1**.

Table 1. Experimental sensitivities for free sensor with the structure shown in **Fig. 2**

Sensor No.	Gauge length of the sensor (mm)	Longitudinal axial strain sensitivity S_{axial} , (rad/mm)
1	120	102.7
2	102	108.7
3	115	105.4
4	117	104.4
5	112	106.8
average		106
Standard deviation		2

3.2 Experimental results from the transverse compression tests

When a bare fibre polarimetric sensor is under transverse compression load, the longitudinal strain in the optical core is assumed to be zero [6]. The relationship between the strains in the optical fibre and the applied load can be obtained from elasticity solutions for a rod of diameter d, under diametrical compression by an average load P [6], which are:

$$\begin{aligned} \varepsilon_2^L &= \frac{1}{E}\left[(1-\nu^2)\frac{2P}{\pi d} - \nu(1+\nu)(-\frac{6P}{\pi d})\right] \\ \varepsilon_3^L &= \frac{1}{E}\left[(1-\nu^2)(-\frac{6P}{\pi d}) - \nu(1+\nu)\frac{2P}{\pi d}\right] \end{aligned} \quad (6)$$

where ε_2^L and ε_3^L are transverse strains (note: ε_2^L is in direction of loading) in the rod, E is the Young's modulus and ν is the Poisson's ratio of the rod. P is load per unit length on the rod and is defined as:

$$P = \frac{F}{L} \quad (7)$$

where F is the force on the rod and L is the length of the rod under compression.

When the optical sensor is rotated, as shown schematically in **Fig. 6**, the relative orientation of the stress rods to the loading direction will change and with them the optical axes of the sensor. Consequently, the strain state in the optical core will change with the rotation of the fibre and hence the sensitivity of the sensor will change with rotation of the sensor.

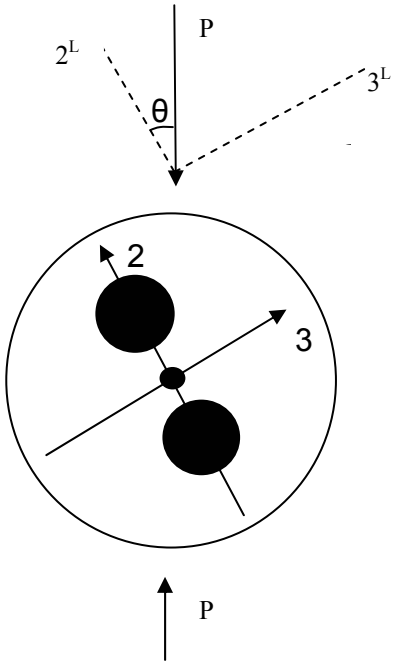

Fig. 6 A schematic diagram showing the transverse loading direction and the optical axes of the optical sensor.

For example, **Fig. 7** shows optical fringes from the same sensor. **Fig. 7(a)** shows the change in output for the ten loading steps followed by the ten unloading steps, and the same is shown in **Fig. 7(b),** except that **t**he sensor has been rotated through 30° in **Fig. 7(b**) compared to **Fig. 7(a)**. There were about 10 seconds of unchanging optical signals between the loading and unloading fringes in **Fig. 7**, corresponding to a time gap between loading and unloading of the weights. A clear optical change induced by each step of manual loading can be seen in the two sets of results, although the fringes are not very regular in form due to the manual loading/unloading.

The transverse sensitivity, S_{trans}, of the sensor under compression can be defined as [5]:

$$S_{trans} = \frac{1}{L}\frac{\Delta\varphi}{\Delta P} \tag{8}$$

where ΔP is the change of load per unit length on the sensor, $\Delta\varphi$ is the phase change induced by ΔP and L is the length of the sensor under transverse compression. Hence, the transverse sensitivity was measured as a function of angle, θ.

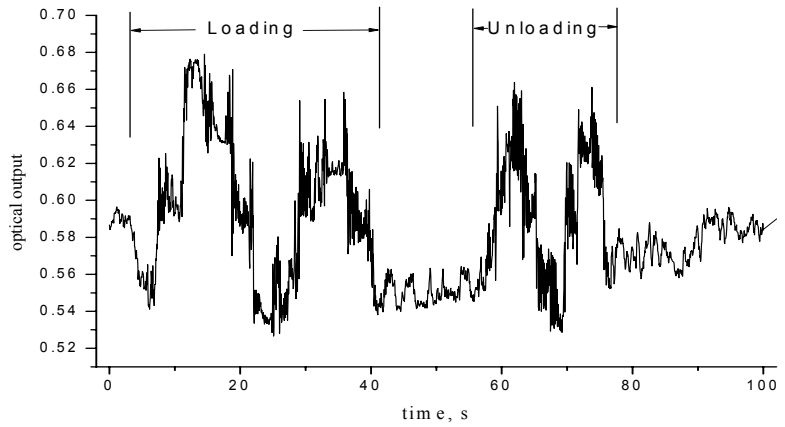

(a)

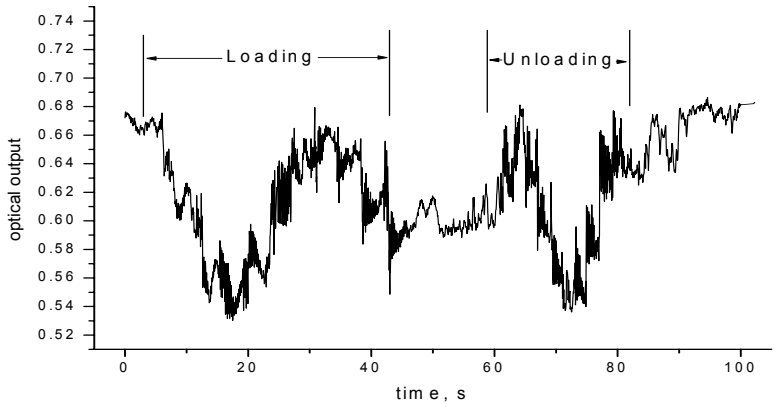

(b)

Fig.7 Optical fringes of a bare sensor under transverse compression.

The results showing the change of sensitivity with rotation angle, θ (as defined in **Fig. 6**) are plotted in **Fig. 8**. The sensitivity as a function of angle shows four peaks, which means that the sensor is more sensitive when loaded parallel to the optical axes. The position of the origin (i.e. 0^0) on the x-axis of **Fig. 8** has been fixed to correspond with the sensor orientation when a line connecting the centre of the SAPs is parallel to the direction of the applied compressive load (see below). Peaks labeled A and B correspond to angles of 0^0 and π. Peaks labeled C and D correspond to angle of $\pi/2$ and $3\pi/2$. The dashed line indicates the trend of the data. The variation in transverse sensitivity with angle is similar to the results found by Sirkis and Lo [5] for a polarimetric sensor fabricated using Bow-tie fibre.

4 Derivation of the strain-optical parameters K_1, K_2 and K_3

The results from the compression tests can be used in conjunction with the results from the tensile tests to obtain the values of K_1, K_2 and K_3.

Assuming that the longitudinal strain is zero for the transverse compression tests [5], then combining Eq.(8) and Eq.(1) gives:

$$S_{trans} = \frac{1}{L}\frac{\Delta\varphi}{\Delta P} = \frac{2\pi}{\lambda}(\varepsilon_2 K_2 + \varepsilon_3 K_3) \tag{9}$$

where ε_2 and ε_3 are strains in directions 2 and 3 in the optical fibre core, as defined in **Fig. 6**.

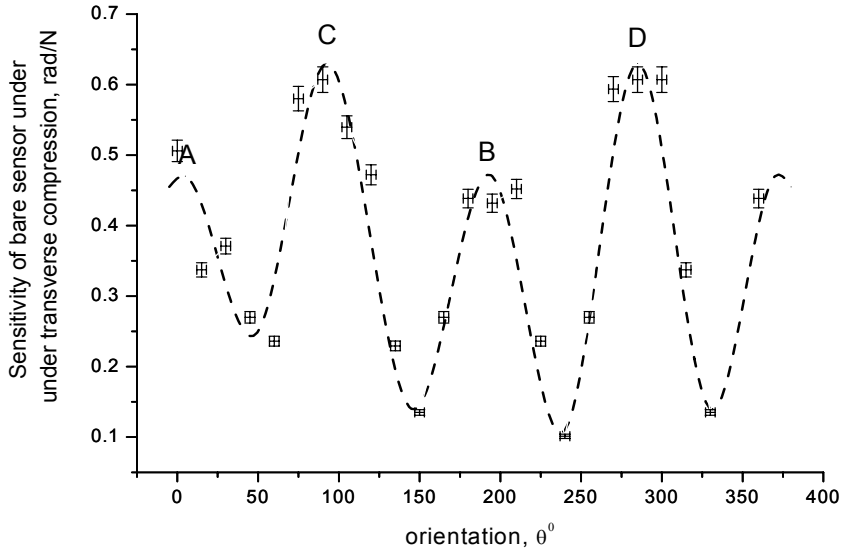

Fig.8 Compression sensitivity as a function of angle θ.

When the sensor rotates by an angle θ relative to the applied transverse compression load direction such that the angle θ is 0 or π, the strains in the optical axis direction-2 and optical axis direction-3 in the core are:

$$\begin{aligned} \varepsilon_2 &= \varepsilon_2^L \\ \varepsilon_3 &= \varepsilon_3^L \end{aligned} \tag{10}$$

When θ is $\pi/2$ or $3\pi/2$, the strains in the optical axis-2 and optical axis-3 in the optical core are:

$$\begin{aligned} \varepsilon_2 &= \varepsilon_3^L \\ \varepsilon_3 &= \varepsilon_2^L \end{aligned} \tag{11}$$

Substituting Eq.(10) and Eq.(11) into Eq.(9), the sensitivity of the sensor under transverse compression at these four angles can be expressed as [5]:

$$\begin{aligned} S_{trans}^{0,\pi} &= \frac{2\pi}{\lambda}(\varepsilon_2^L K_2 + \varepsilon_3^L K_3) \\ S_{trans}^{\frac{\pi}{2},\frac{3}{2}\pi} &= \frac{2\pi}{\lambda}(\varepsilon_3^L K_2 + \varepsilon_2^L K_3) \end{aligned} \tag{12}$$

There are three components of a PANDA fibre, the SAPs (also called stress rods), the optical fibre core and the cladding. The materials of the stress rods have the highest thermal expansion coefficients and during the cooling procedure of manufacture, the stress rods contract more than the other parts. Hence, the residual strain in the optical core in the 2-direction is positive (tensile) and the residual strain in the 3-direction is negative (compression). When the optical axis-2 of the optical core is under compression, which means θ in **Fig. 6** is 0 or π, the residual strain in the core in the direction-2 is reduced, and the birefringence (difference in propagation constants between directions -2 and -3) is reduced.

Hence, the sensitivity of the sensor is relatively low. This corresponds to the two lower peaks in **Fig. 8**, labeled as A and B. When the optical axis-2 of the optical core is under tension, which means θ in **Fig. 6** is *π/2* or *3π/2*, the difference in strain in the core between the 2-direction and 3-direction is enhanced, and the sensitivity of the sensor is relatively high. This corresponds to the two higher peaks in **Fig. 8**, labeled as C and D.

The material properties of the optical fibre are shown in **Table 2** from [3]. The numerical values for the sensitivity at the peaks for angles of *0*, *π* and *π/2*, *3π/2* are 0.47 rad/mm and 0.63 rad/mm respectively. Substituting these values into Eq.(5) and Eq.(12), the resulting numerical equations are:

$$\begin{bmatrix} K_1 - 0.154K_2 - 0.154K_3 = 0.01 \\ -4.99K_2 + 2.42K_3 = 0.47 \\ 2.42K_2 - 4.99K_3 = 0.63 \end{bmatrix} \tag{13}$$

After solving the equations, the *K*-values of the polarimetric sensor based on the PANDA fibre are found to be:

$$\begin{bmatrix} K_1 = -0.055 \\ K_2 = -0.204 \\ K_3 = -0.225 \end{bmatrix} \tag{14}$$

Table 2 Optical fibre properties [3]

Property	Value
Young's modulus, E (GPa)	73.3
Poisson's ratio, ν	0.154
Diameter of the optical fibre, d (μm)	125

The *K*-values found here are compared with the K values for a polarimetric sensor based on Bow-tie fibre in **Table 3**. It is clear that the parameters for the PANDA fibre are smaller than those for the Bow-tie fibre, which is in good agreement with Tsai et al [7] who found that a polarimetric sensor based on PANDA fibre is less sensitive to longitudinal strain than the Bow-tie fibre. Interestingly, although both PANDA and Bow-tie fibres are more sensitive to transverse strain than longitudinal strain (i.e. K_2 and K_3 are both larger than K_1), it is clear that greater transverse sensitivity can be achieved using the Bow-tie fibre.

5. Conclusion

The strain-optical parameters of a PANDA fibre have been determined and found to be K_1 = -0.055, K_2 = -0.204 and K_3 = -0.225. These results suggest that a polarimetric sensor based on PANDA fibre has a lower transverse strain sensitivity than a similar sensor based on Bow-tie fibre.

Table 3 Model parameters for polarimetric sensors based on PANDA or Bow-tie fibres.

Fibre	K_1	K_2	K_3
PANDA	-0.055	-0.204	-0.225
Bow-tie	-0.197	-0.714	-0.618

Reference

1**. Wang H**., **Ogin S.L**., **Thorne A.M**., .**Reed G.T** and **Ussorio M**.. "Crack detection around a hole in a cross-ply laminate using an embedded polarimetric fibre optic sensor," in "Proceeding of ICCM-14, The Fourteenth International Conference on Composite Materials", San Diego, USA; July, 2003.

2**. Wang H**., **Ogin S.L**., **Thorne A.M** and **Reed G.T**. "Use of a polarimetric sensor for damage detection in cross-ply composite laminate," in "Proceedings of ECCM-10, The Tenth European Conference on Composite Materials" – Brugge, Belgium, June 2002.

3**. Sirkis J. S**. "Unified approach to phase-strain-temperature models for smart structure interferometric optical fibre sensors: Part 1, Development, Part 2, Application", Optical Engineering. **324**(1993); pp. 752-773.

4. **Lo Y. I**., **Sirkis J. S**. and **Ritchie K. T**. "A study of the optomechanical response of a diametrically loaded high-birefringent optical fibre", Smart Materials and Structure, **4**(1995); pp. 327-333.

5. **Sirkis J.S**. and**. Lo Y.L**.. "Phase-strain model for polarimetric strain sensor based on fictitious residual strains". Journal of Intelligent Materials Systems and Structures, **5**(1994); pp.494-500.

6. **Timoshenko S**. and **Goodier J.** "Theory of elasticity", McGraw-Hill, New York, 1982

7. **Tsai K**., **Kim K**, and **Morse T**. "General solutions for stress-induced polarisation in optical fibres", Journal of lightwave technology, **9**(1991), pp. 7-17